Supporting Information for

Disorder-free conformation boosts phonon and charge transfer in Electron-Deficient-Core-Based non-fullerene acceptor

Chujun Zhang[1†], Jun Yuan[2,3†], Ka Lok Chiu[1], Hang Yin[1], Weifang Liu[2], Guanhaojie Zheng[3], Johnny Ka Wai Ho[1], Suzhen Huang[4], Gaoxing Yu[4], Feng Gao[3], Yingping Zou[2], Shu Kong So[1★].

[1]Department of Physics and Institute of Advanced Materials, Hong Kong Baptist University, Kowloon Tong, Hong Kong SAR, P.R. China

[2]College of Chemistry and Chemical Engineering, Central South University, Changsha 410083, Hunan, P.R. China

[3]Department of Physics, Chemistry and Biology (IFM), Linköping University, Linköping 58183, Sweden

[4]Key Laboratory of Interfacial Physics and Technology, Shanghai Institute of Applied Physics, and Shanghai Synchrotron Radiation Facility, Zhangjiang Laboratory, Chinese Academy of Sciences, Shanghai 201204, China

[5]These authors contributed equally

★e-mail: skso@hkbu.edu.hk;

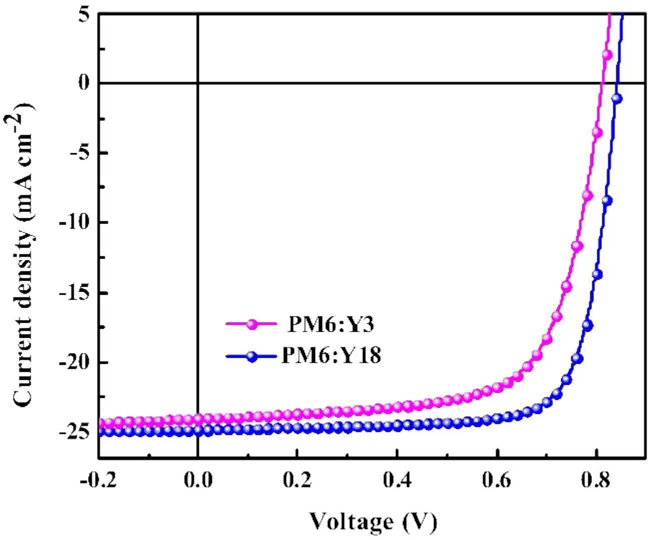

Supplementary Figure S1 | Photovoltaic characteristic: J-V curves of the PM6:Y3 and PM6:Y18 solar cell devices with inverted architectures.

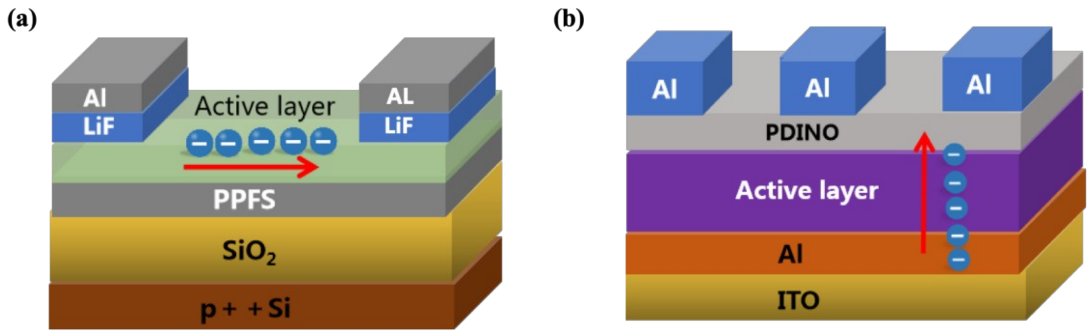

Supplementary Figure S2 | Schematic diagram and electron transport direction of (a) n-type FET device and (b) electron-only device.

Supplementary Figure S3 (a) and (b) show the measured frequency dependent capacitances at selected applied electric field strengthen for the two BHJ blends. In each data set, the position of the drop of capacitance is correlated with the carrier transit time. The AS mobility at a certain electric field can be extracted from the negative differential susceptance -ΔB vs f plot [as shown in the insets of Fig S3(a) and (b)]. If the minimum capacitance C_{min} occurs at higher frequency, it indicates a higher carrier mobility. Therefore, μ_e in PM6:Y18 is higher than that of PM6:Y3 in all electric fields (full spectra of AS signal can be found in Supplementary Figure S4).

The electric field range between open-circuit condition ($F=0$) to short-circuit condition ($F_{Jsc} = V_{oc}/d$, d is the sample thickness) was defined to characterize the device relevant mobilities in BHJ blend. In our case, the V_{oc} of the Y3 and Y18 based solar cell device is around 0.81-0.84V, and the optimized active layer thickness is around 100 nm. Therefore, the square root of applied electric field region of the PM6 based devices is $\sqrt{V/d} \approx 288(V/m)^{1/2}$. The electric field between $F^{1/2} = 0$ to $F^{1/2} = 288$ (V/cm)$^{1/2}$ is the device relevant.

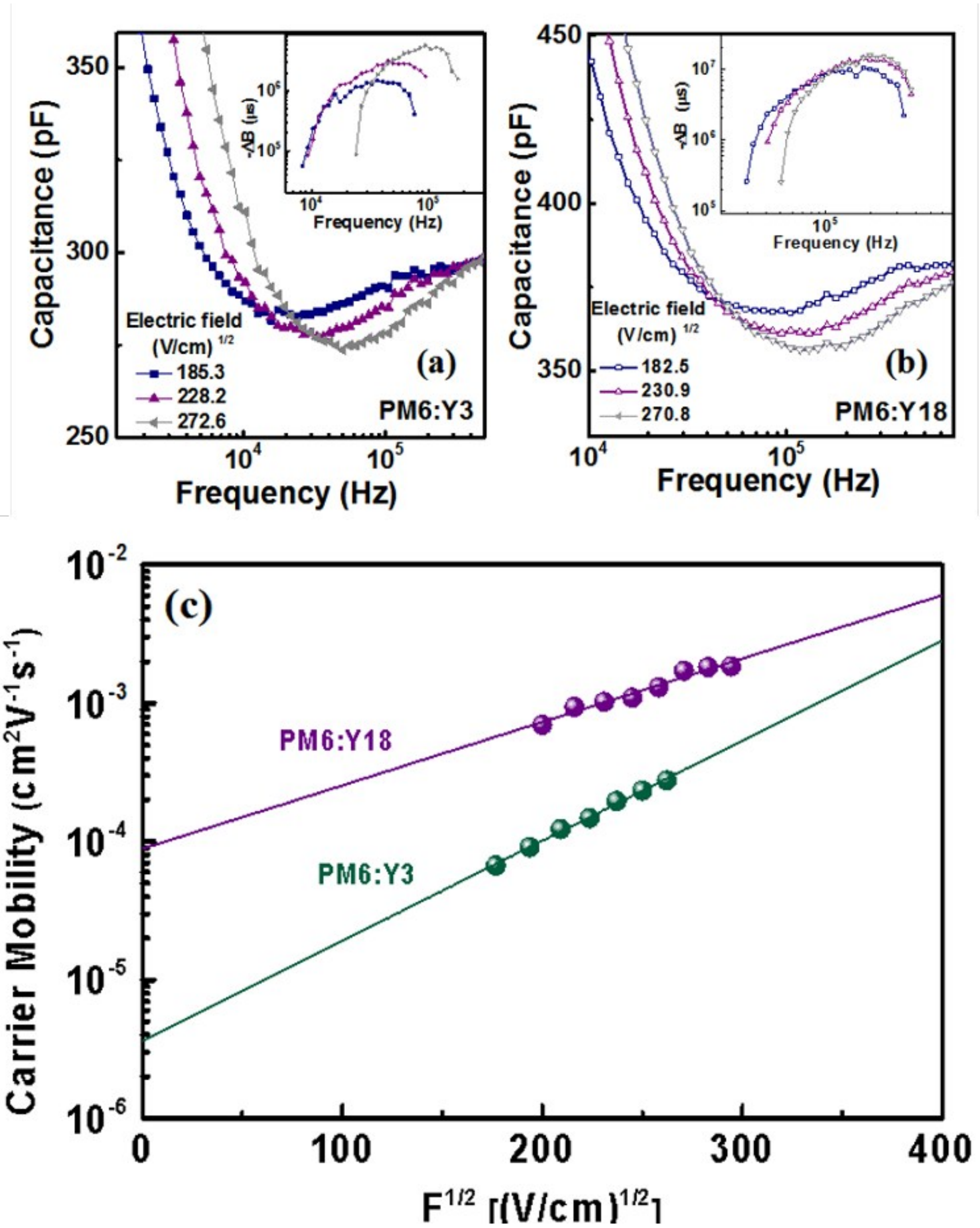

Supplementary Figure S3 | Admittance spectroscopy for frequency-dependent capacitance at different electric field for **(a)** PM6:Y3 and **(b)** PM6:Y18. Inset is the negative susceptance vs frequency plot for PM6:Y3 and PM6:Y18 which the carrier transit times and field dependent electron mobilities are derived. **(c)** Field dependent electron mobilities of PM6:Y3 and PM6:Y18. The spheres represent the data extracted from AS measurements. The solid lines are the best fit of mobility data. The value of $\mu_{0,e}$ and β_e can be extracted from the plot. The electric field between 0 to 288 (V/cm)$^{1/2}$ is the device relevant region, where 0 (V/cm)$^{1/2}$ is open-circuit condition and 288 (V/cm)$^{1/2}$ is short-circuit condition.

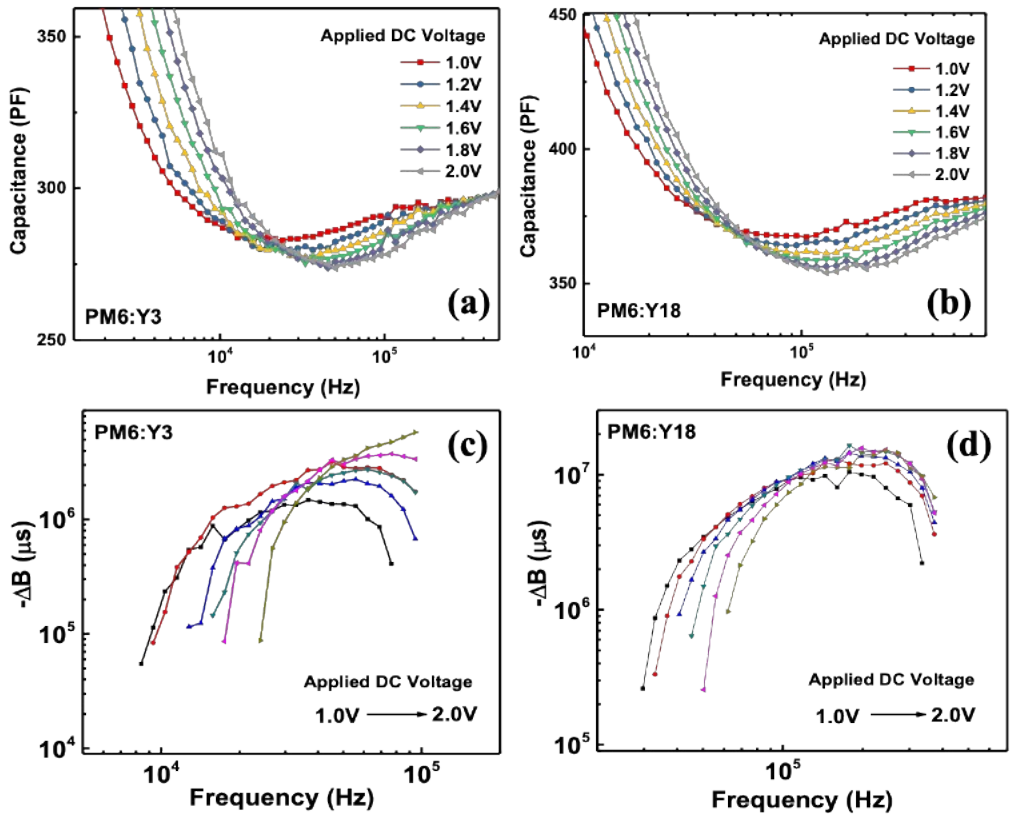

Supplementary Figure S4 | Frequency-dependent capacitance at different electric field for **(a)** PM6:Y3 and **(b)** PM6:Y18. The negative susceptance vs frequency plot for **(c)** PM6:Y3 and **(d)** PM6:Y18 which the carrier transit times and field dependent electron mobilities are derived.

TFT fabrication and measurement. The silicon wafers were cleaned by deionized water,acetone and isopropanol for 15 min and then put the substrate under UV-treatment for 13min. PPFS dissolved in methyl isobutyl keton （2,2'-Azobis (2-methylpropionitrile), ethyl isobutyl ketone）(10mg/ml) was spun on the substrates at 2000rmp for 60s. The thickness is about 30nm. The PM6:acceptor BHJ layers was spin-coated on the top after the PPFS films annealed at 120℃for 2 hours. The thickness of the active layer is about 110nm. After that the substrates with BHJs were then transferred into a high vacuum chamber (~4×10^{-6} torr) and evaporated a 1nm LiF and 100nm aluminu, forming a channel length of 50μm. Measurements was done in cryostat (Oxford Instruments,Optistat DN-V) at vacuum below 10^{-4} torr and dark conditions. Keithley 236 source measurement unit together with a Xantrex XT 120-0.5 as the DC gate voltage supply. The saturation mobilities of OTFT were calculated from the transfer characteristics by: $I_{DS} = \frac{W}{2L} C_i \mu_{sat} (V_G - V_T)^2$, where I_{DS} is the source drain current, W and L are the TFT channel width and length, C_i is the capacitance per unit of the dielectric material, μ_{sat} is the carrier mobility, V_G is the gate voltage and V_T is the threshold voltage.The electron-only device structure is given in Supplementary Figure S2 (a).

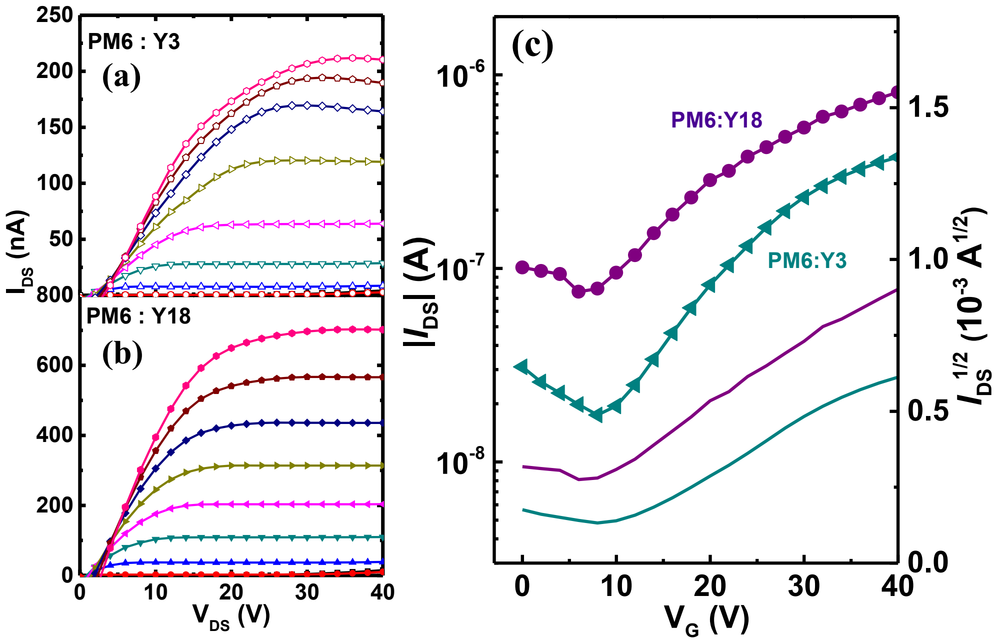

Supplementary Figure S5 | Out-put characteristics of n-type bottom-gate-top contact FET using **(a)** PM6:Y3 and **(b)** PM6:Y18. **(c)** Transfer characteristics of FET device. The μ_{sat} of corresponding films can be extracted by following equation $I_{DS} = \frac{W}{2L} C_i \mu_{sat} (V_G - V_T)^2$.

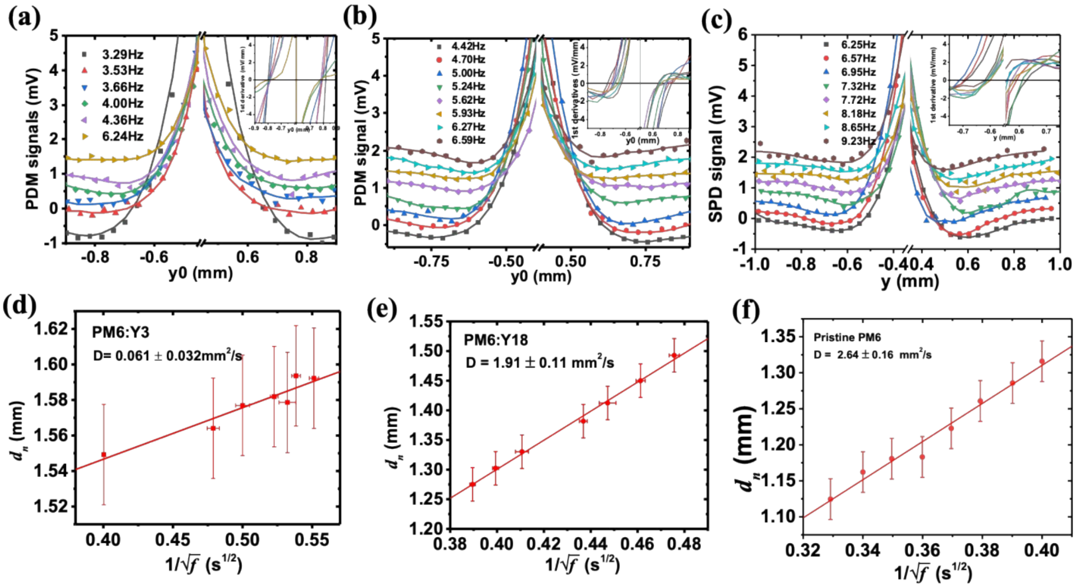

Supplementary Figure S6 | Scanning photothermal deflection (SPD) signals at different frequency of **(a)** PM6:Y3, **(b)** PM6:Y18 blend film and **(c)** Pristine polymer film. Insets represent the 1st derivation of SPD signals at different frequency. Variations of normalized d_n against $\sqrt{1/f}$ for **(d)** P M6:Y3, **(e)** PM6:Y18 blend film and **(f)** Pristine polymer film.

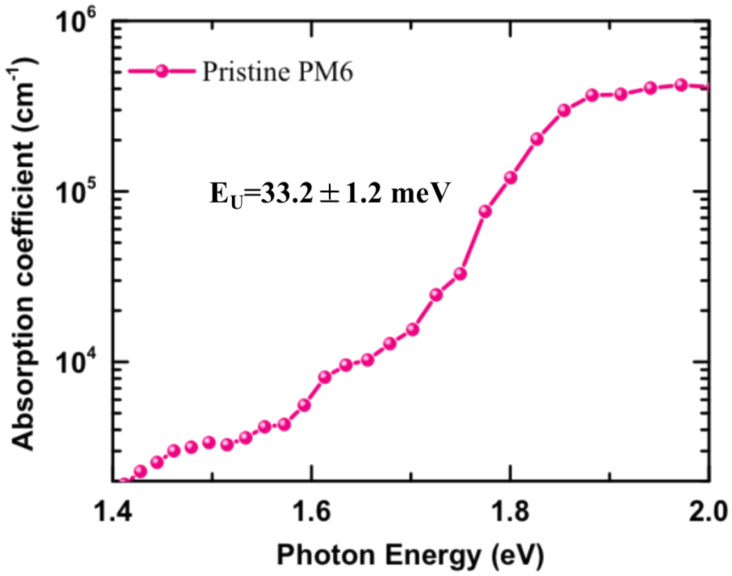

Supplementary Figure S7 | PDS-derived absorption spectra of pristine PM6 film.

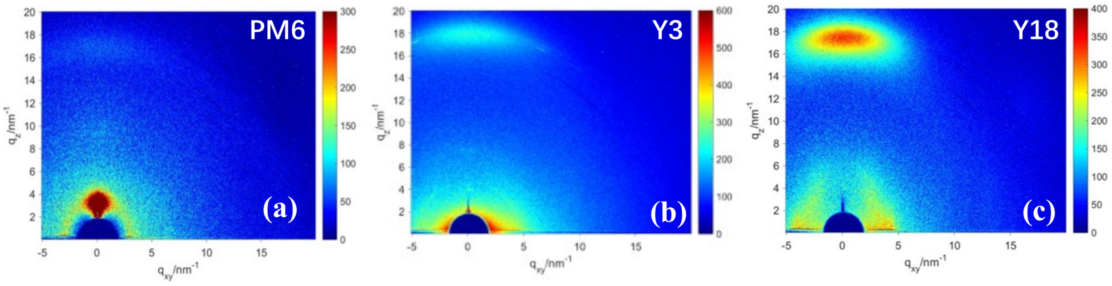

Supplementary Figure S8 | The 2D GIWAXS patterns of the pristine film of (a) PM6 (b) Y3 and (c) Y18.

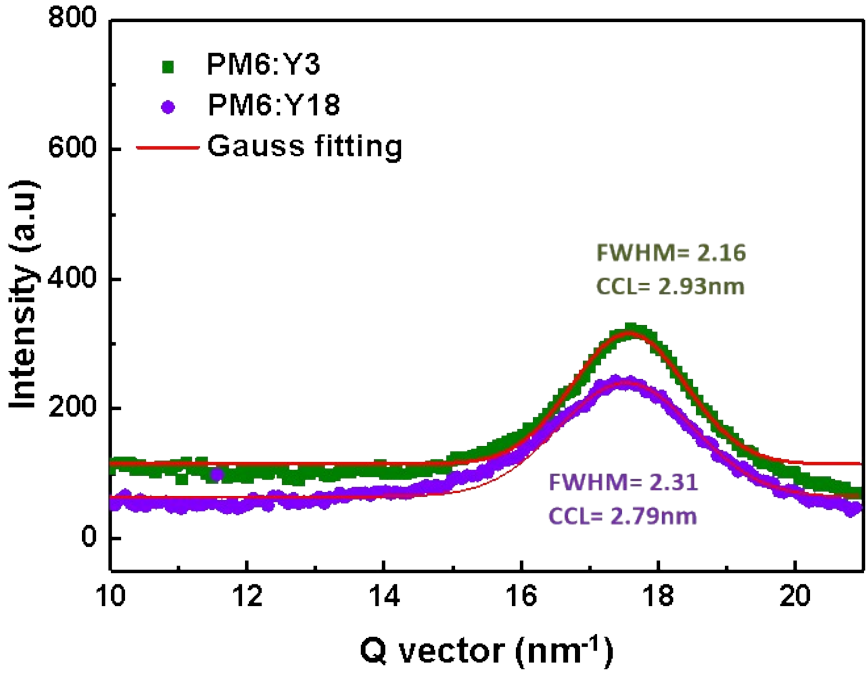

Supplementary Figure S9 | The out-of-plane (OOP) GIWAXS line cut profiles corresponding to PM6:Y3 and PM6:Y18 blend films. The full width at half maximum (FWHM) was obtained from the Gauss fitting. The crystalline coherence length (CCL) is monitored by the FWHM using the Scherrer equation.

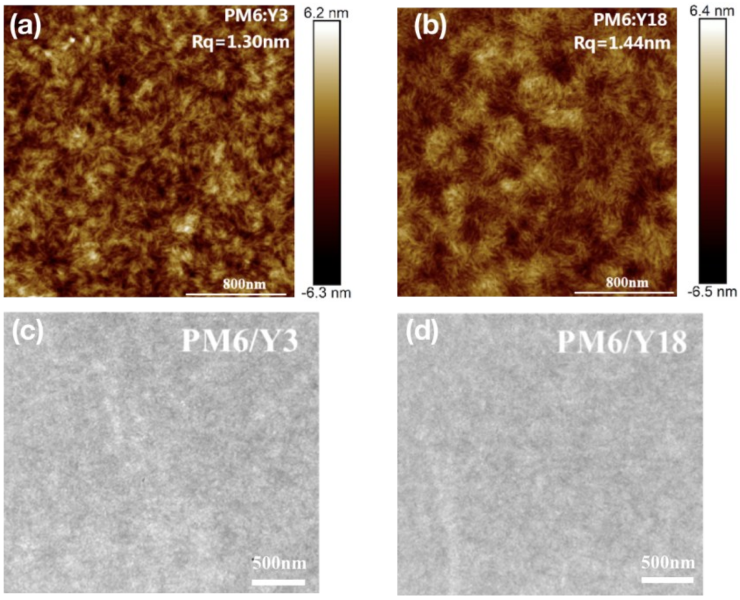

Supplementary Figure S10 | a,b) AFM height images, c,d) TEM images of PM6:Y3 and PM6:Y18 blend film.